ACS MATERIALS LETTERS

www.acsmaterialsletters.org

Paper presentation

Presented by:
Riya Dutta
08.06.2024

A Sandcastle-Worm-Inspired Strategy toward Antimicrobial Fouling and Fireproof Composite

Yu-Xin Lin, Teng Fu,* De-Ming Guo, Ya-Ling Tang, Jie-Hao He, Chuan Liu, Shu-Gen Wu, Bo-Wen Liu, Li Chen, and Yu-Zhong Wang*

Cite This: *ACS Materials Lett.* 2024, 6, 627–639

Read Online

Corresponding Authors

Teng Fu – *The Collaborative Innovation Center for Eco-Friendly and Fire-Safety Polymeric Materials (MoE), National Engineering Laboratory of Eco-Friendly Polymeric Materials (Sichuan), State Key Laboratory of Polymer Materials Engineering, College of Chemistry, Sichuan University, Chengdu 610065, China;* orcid.org/0000-0002-2250-2453; Email: futeng@scu.edu.cn

Yu-Zhong Wang – *The Collaborative Innovation Center for Eco-Friendly and Fire-Safety Polymeric Materials (MoE), National Engineering Laboratory of Eco-Friendly Polymeric Materials (Sichuan), State Key Laboratory of Polymer Materials Engineering, College of Chemistry, Sichuan University, Chengdu 610065, China;* Email: yzwang@scu.edu.cn

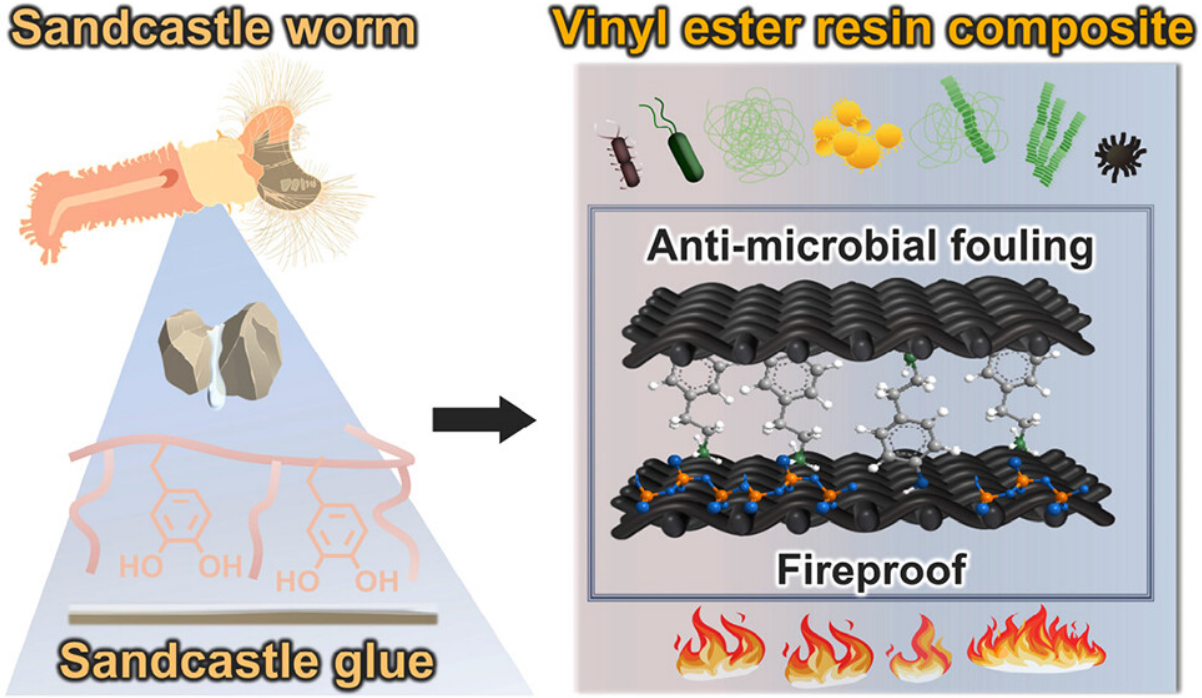

Introduction

Phragmatopoma California
Sandcastle worm

Sandcastle

https://www.inaturalist.org/photos/175054886

Background

The bioadhesive of *Phragmatopoma californica* tubes: a silk-like cement containing L-DOPA

Rebecca A. Jensen and Daniel E. Morse

Department of Biological Sciences and The Marine Science Institute, University of California, Santa Barbara, California 93106, USA

Journal of Comparative Physiology B

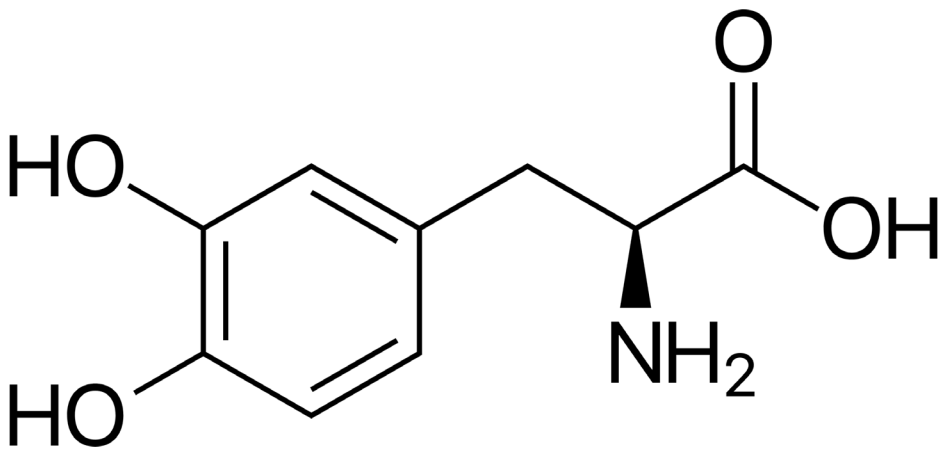

3,4-di-hydroxyphenylalanine

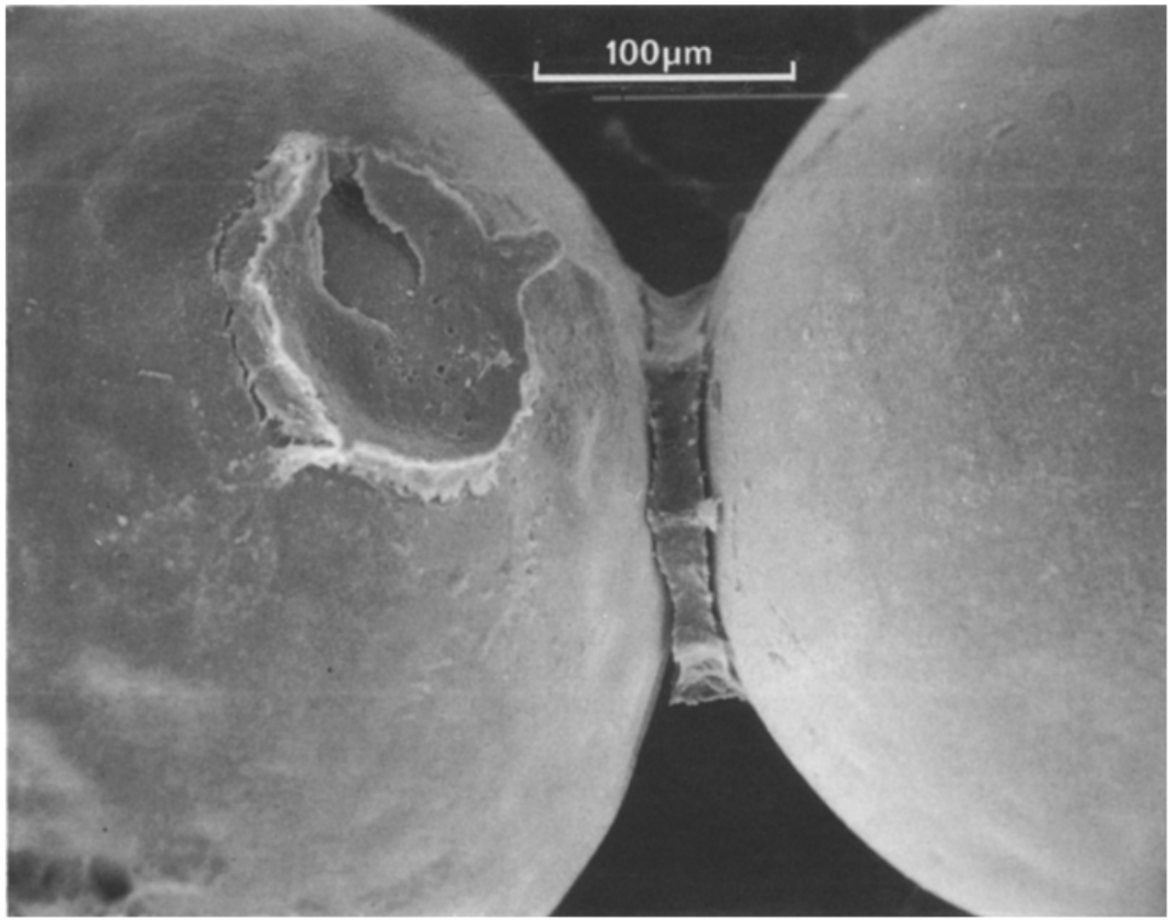

Fig: SEM of glass beads isolated from a tube built in the laboratory by adult *Phragmatopoma californica*

Background

Langmuir **2007,** *23,* 5045−5049

Multiscale Structure of the Underwater Adhesive of *Phragmatopoma Californica*: a Nanostructured Latex with a Steep Microporosity Gradient

Mark J. Stevens, Rebekah E. Steren, Vladimir Hlady, and Russell J. Stewart*

Table 1. Adhesive Set Times with Three Types of Substrate

substrate	average set time (s)
glass microspheres	22.8 ± 7.5 ($n = 85$)
silicon	29.7 ± 5.8 ($n = 32$)
bovine cortical bone	23.5 ± 5.3 ($n = 30$)

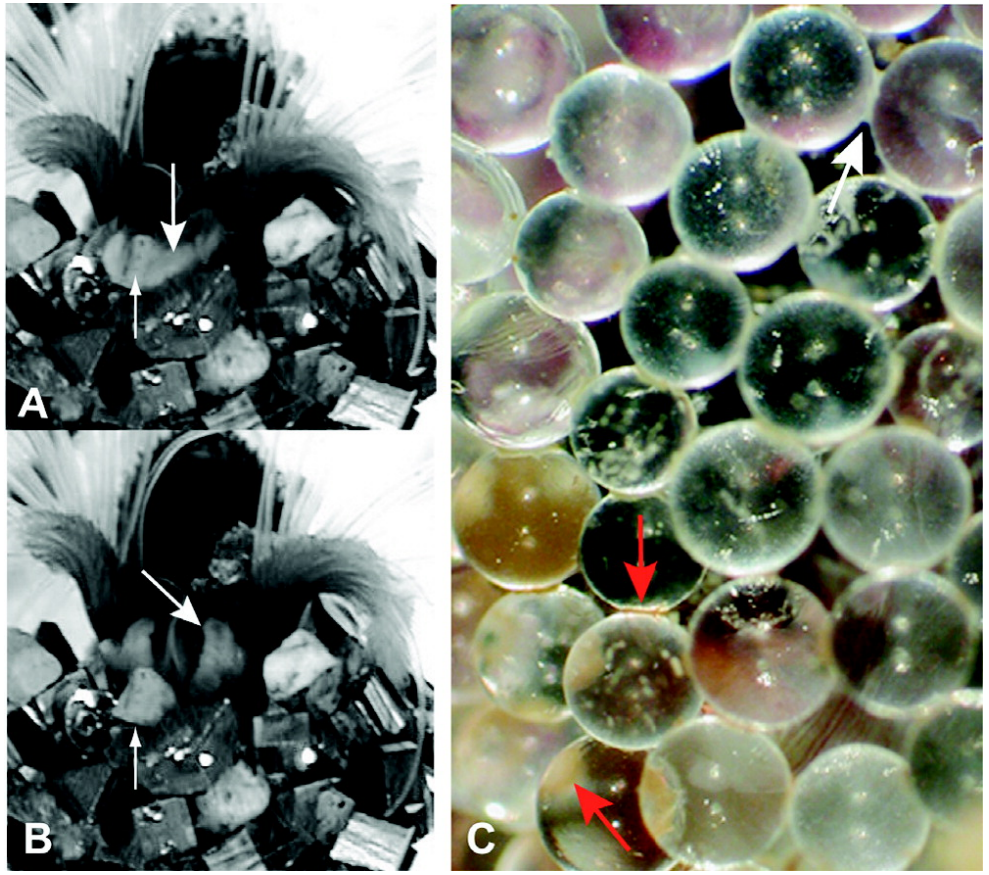

Background

Langmuir **2007,** *23,* 5045−5049

Multiscale Structure of the Underwater Adhesive of *Phragmatopoma ica*: a Nanostructured Latex with a Steep Microporosity Gradient

Stevens, Rebekah E. Steren, Vladimir Hlady, and Russell J. Stewart*

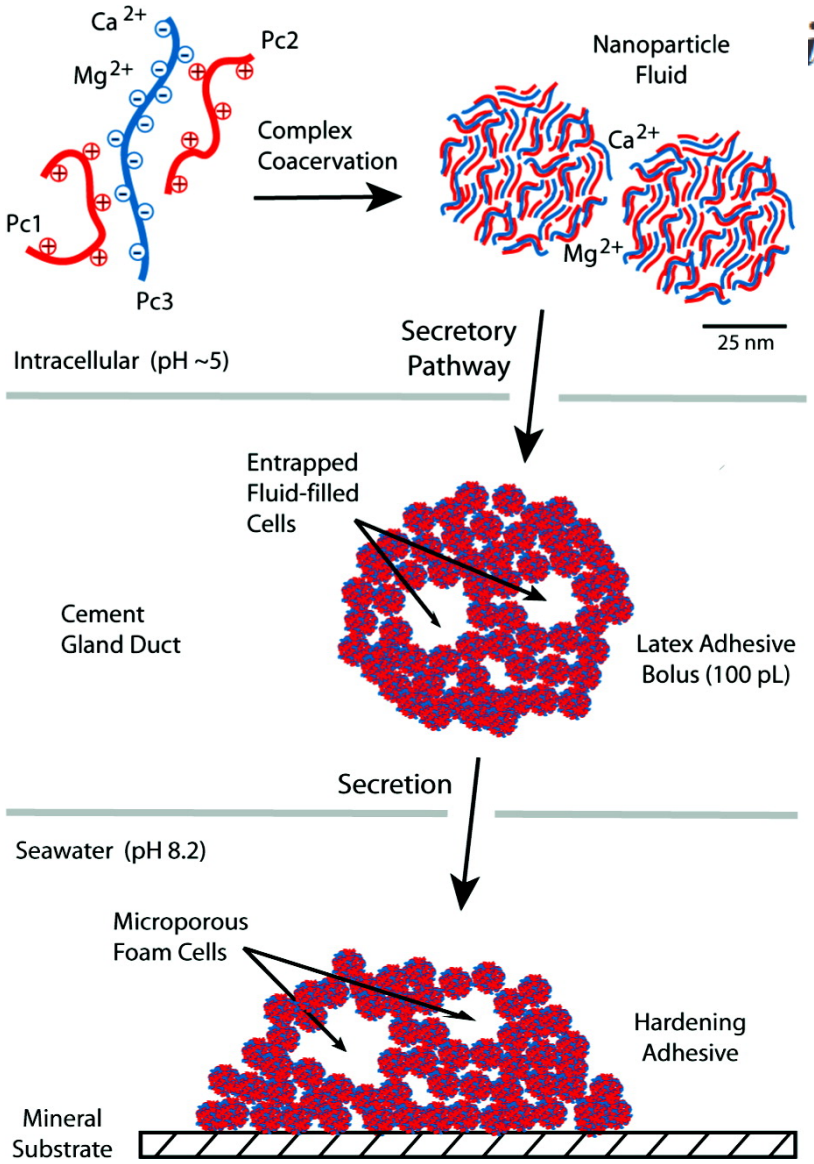

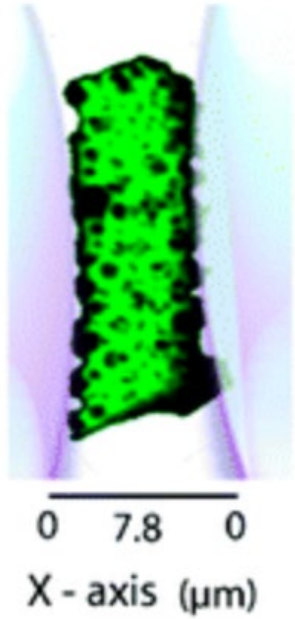

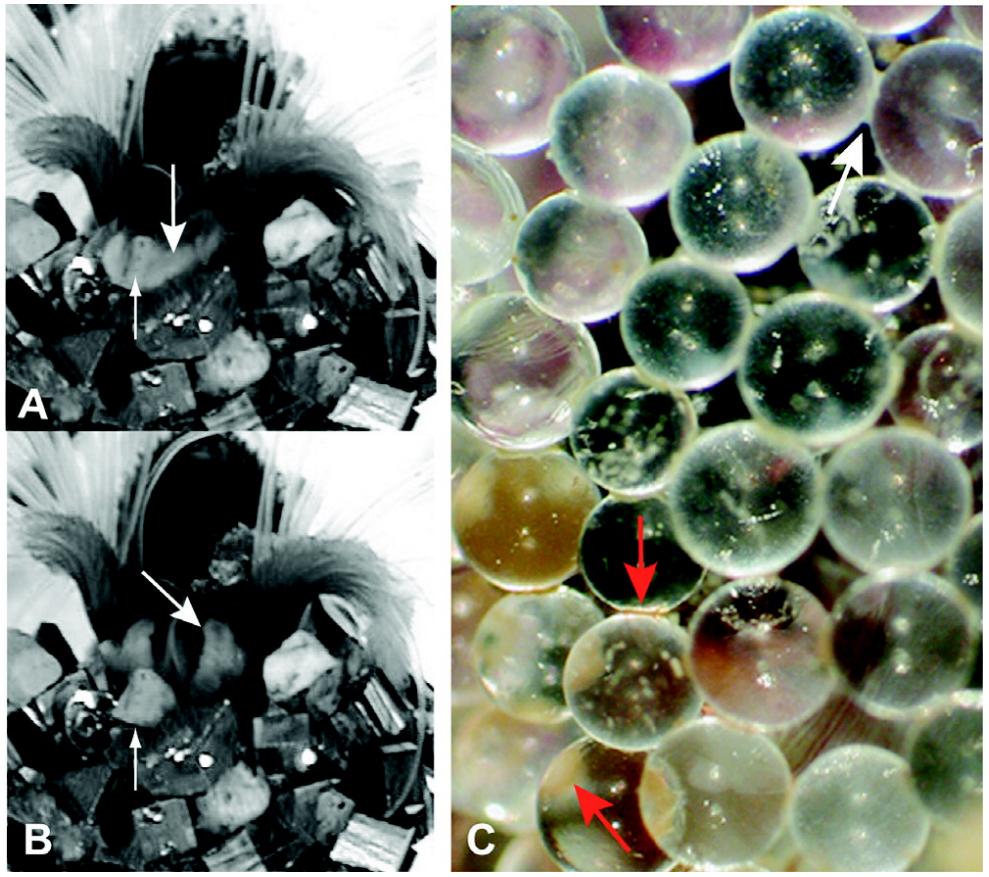

Interesting facts

1. The typical amount of glue the *Phragmatopoma californica* produces is approximately **100 picoliters**.

2. The glue sets in about **30 seconds**, probably triggered by the large difference in acidity between the **acidic glue and seawater**.

Why this paper?

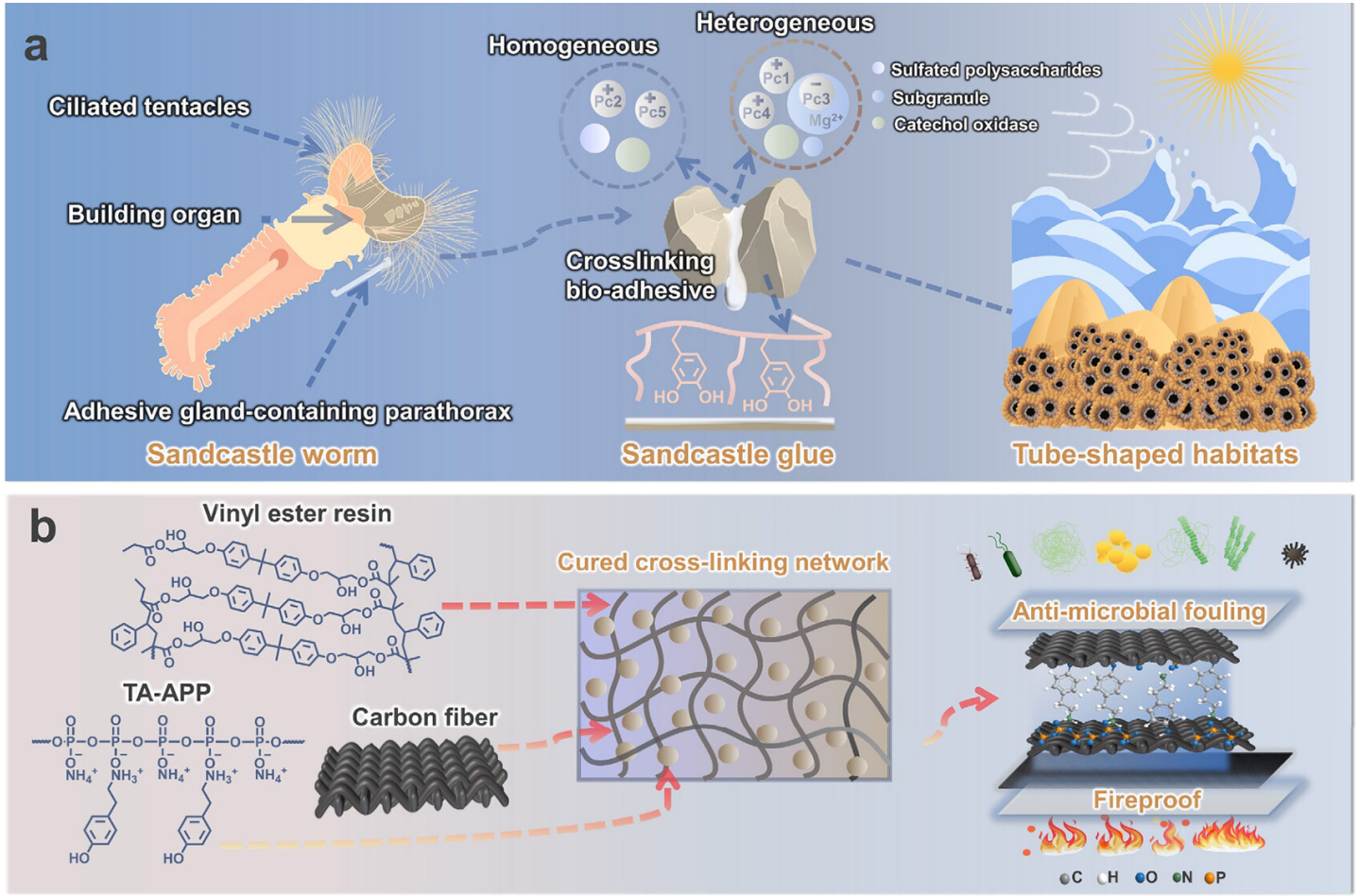

1. This paper is crucial because we are actively searching for an effective sand binder. It will provide us with valuable information and potential solutions for improving the binding process in sand applications.

2. Additionally, the paper offers insights into the interface interactions and chemistry involved in sand binding, which will enhance our understanding of how different binders work and help us optimize our binding strategies.

Material design

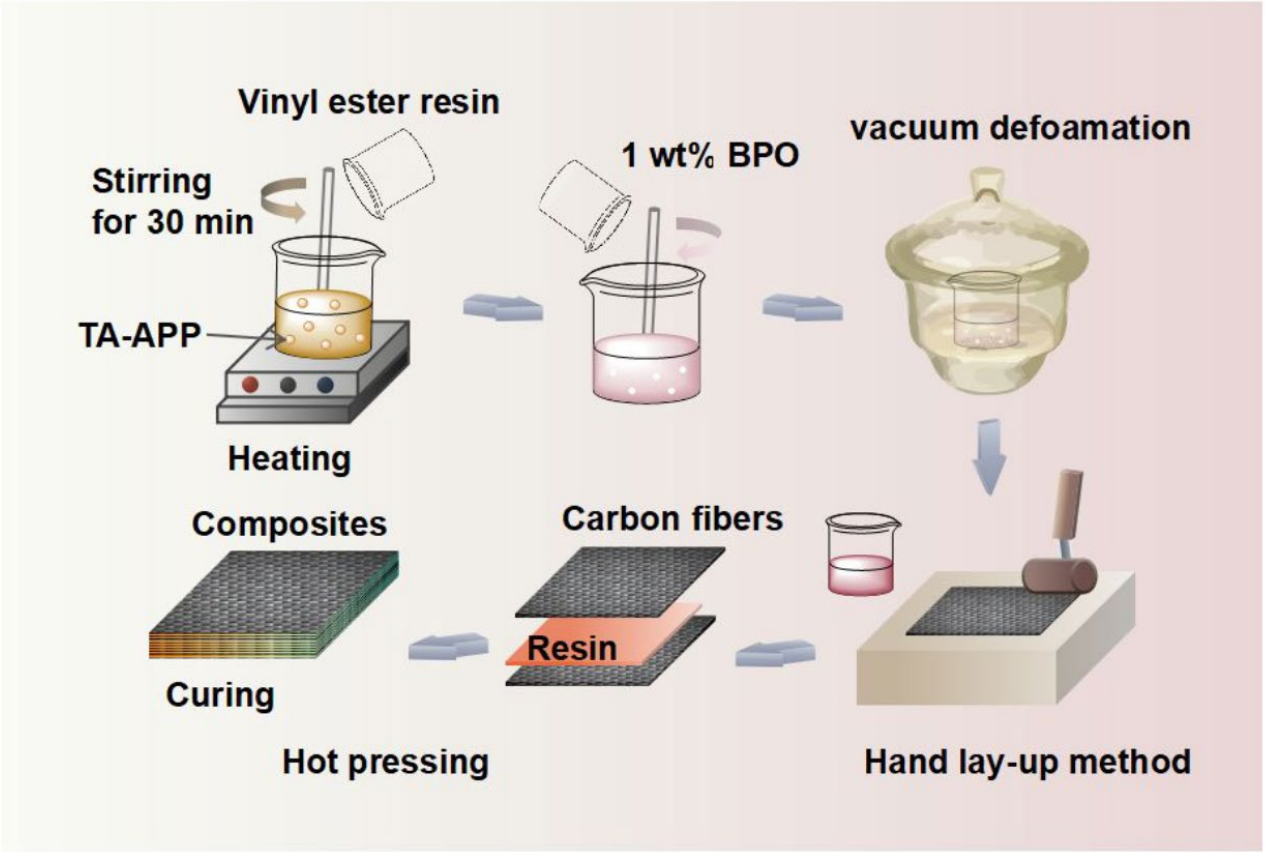

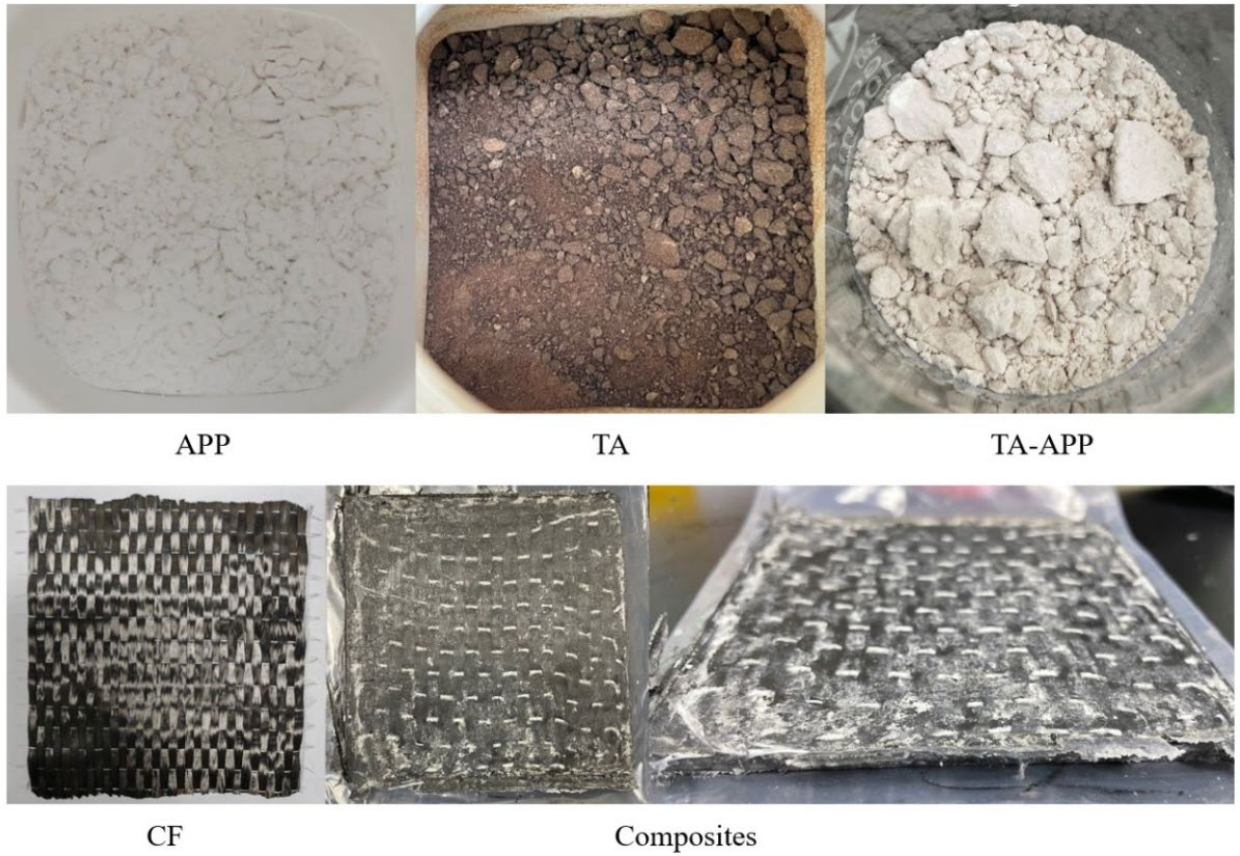

Naming and composition

Table S1. Formula of VER, VAR, VTR, VEC, VAC, VTC.

Samples	VER 901 (wt%)	BPO (g)	APP (wt%)	TA-APP (wt%)	CF (wt%)
VER	100	2	—	—	—
VAR	70	2	30	—	—
VTR	70	2	—	30	—
VEC	50	0.6	—	—	50
VAC	35	0.6	15	—	50
VTC	35	0.6	—	15	50

Experimental data

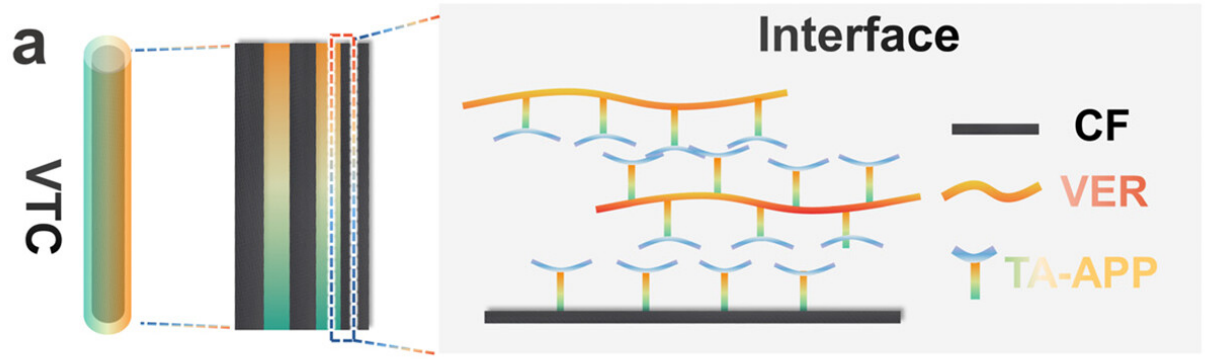

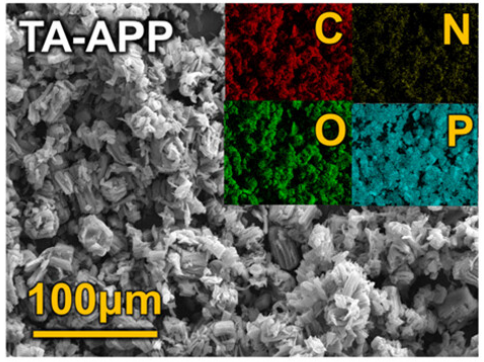

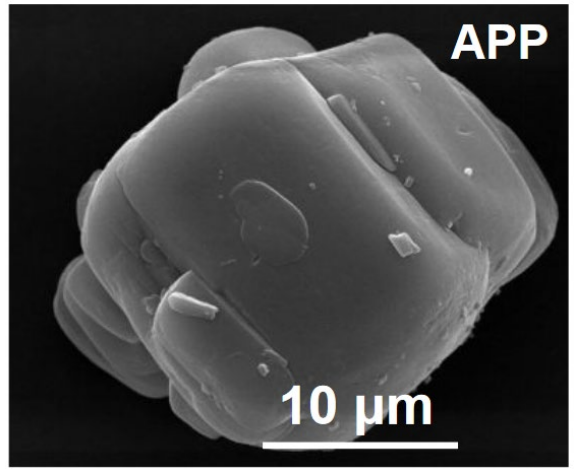

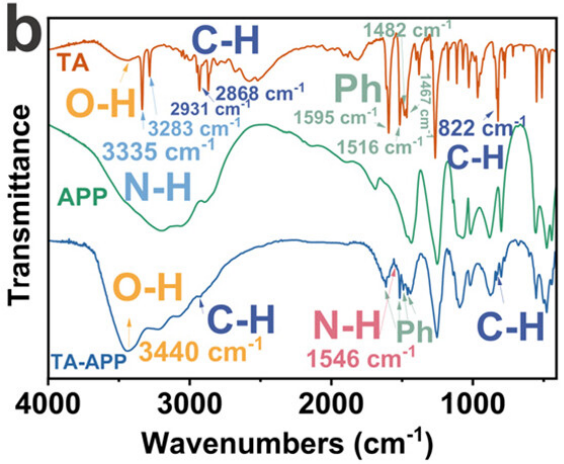

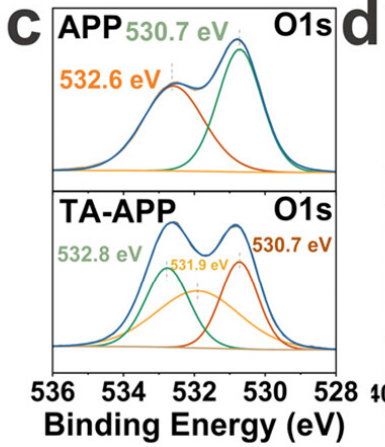

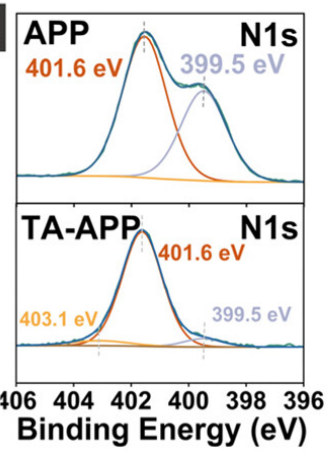

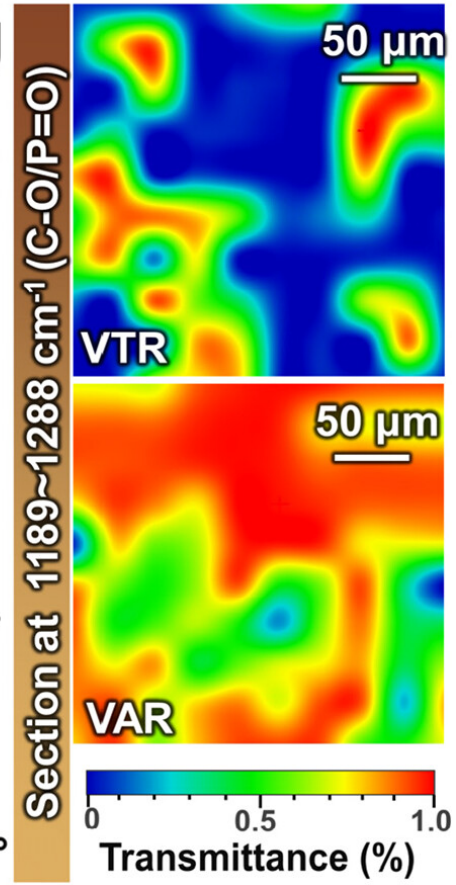

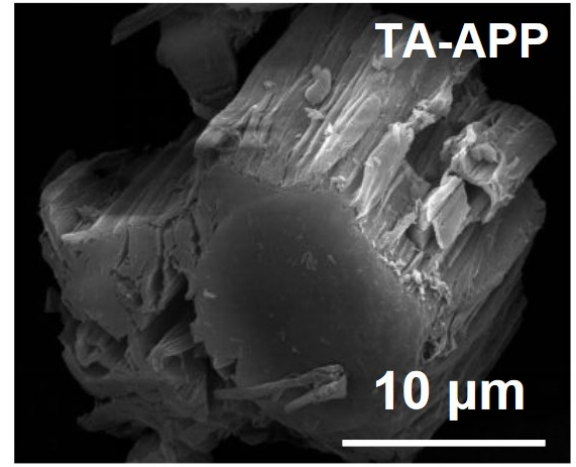

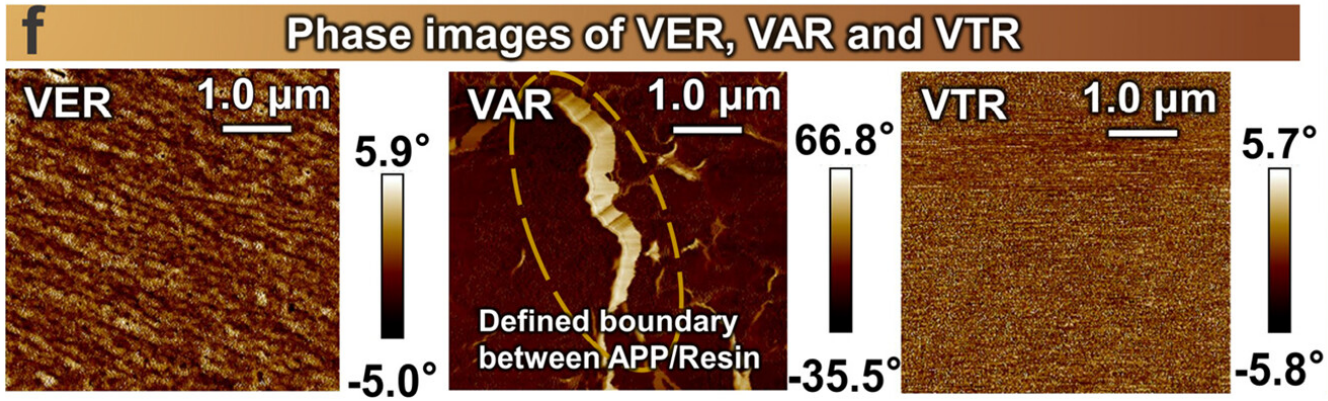

Fig: (a) Multilayer interface construction. (b) FTIR spectra. (c, d) XPS spectra. (e) EDX element mapping images. (f) AFM phase images (imaging area of ~5.0 μm × 5.0 μm). (g) Micro ATR-FTIR images (imaging area of ~0.5 mm × 0.5 mm).

Experimental data

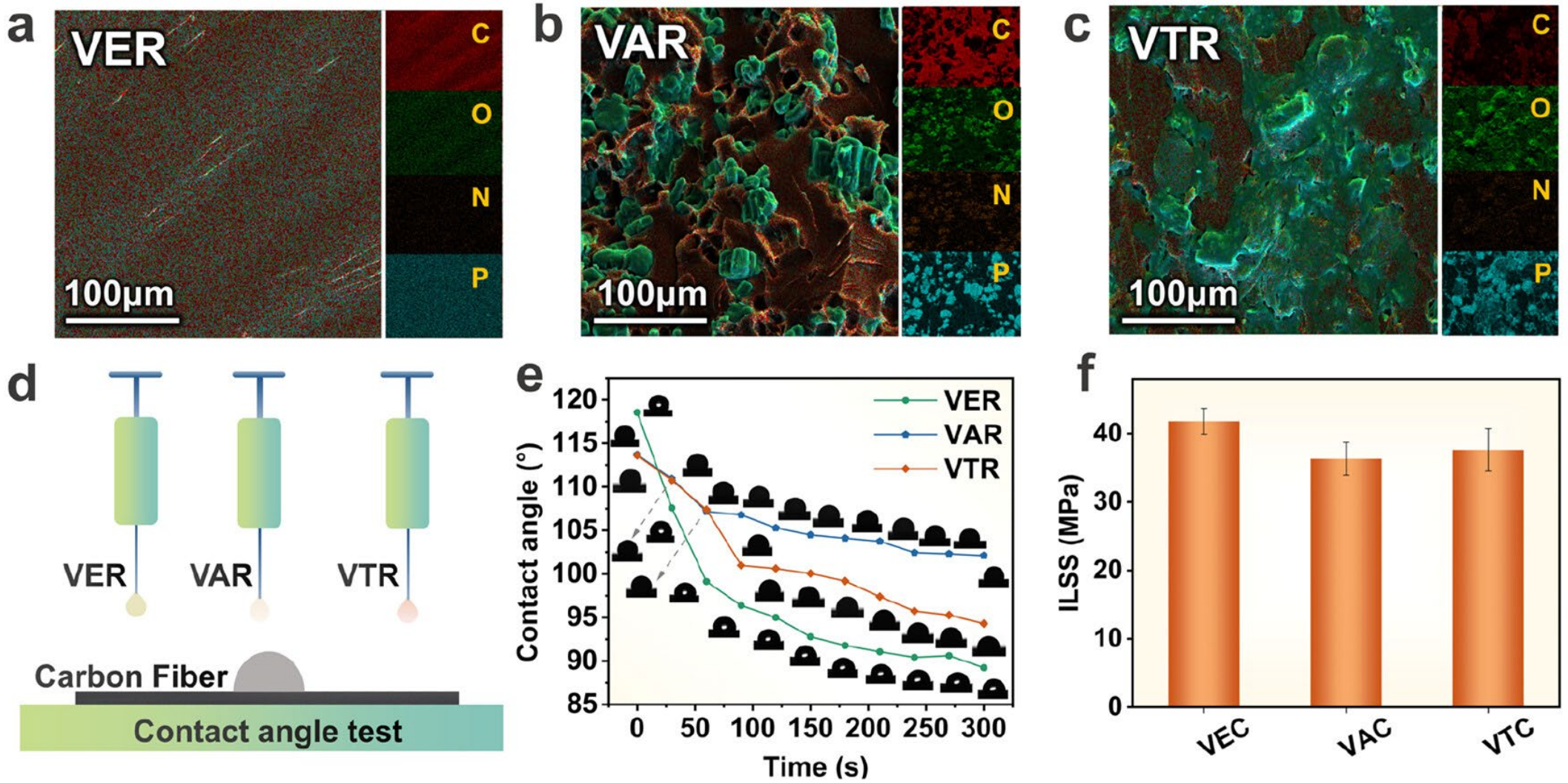

Fig: (a−c) EDX mapping images. (d) Contact angle testing process diagram. (e) The changes in the contact angle on the surface of carbon fibers with time. (f) Interlaminar shear strength.

Experimental data

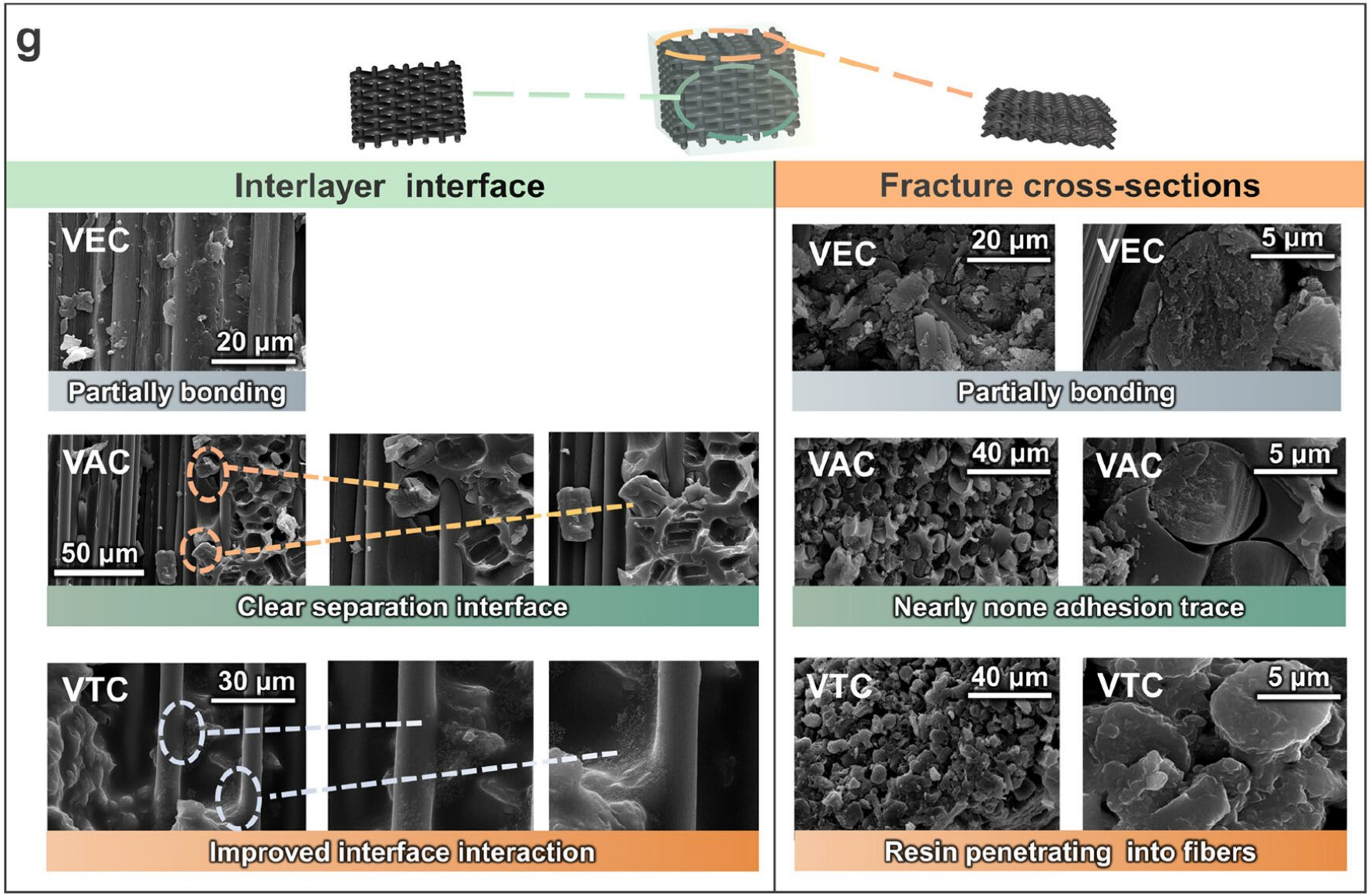

Fig: (g) SEM images of interlaminar section and fracture surface

Experimental data

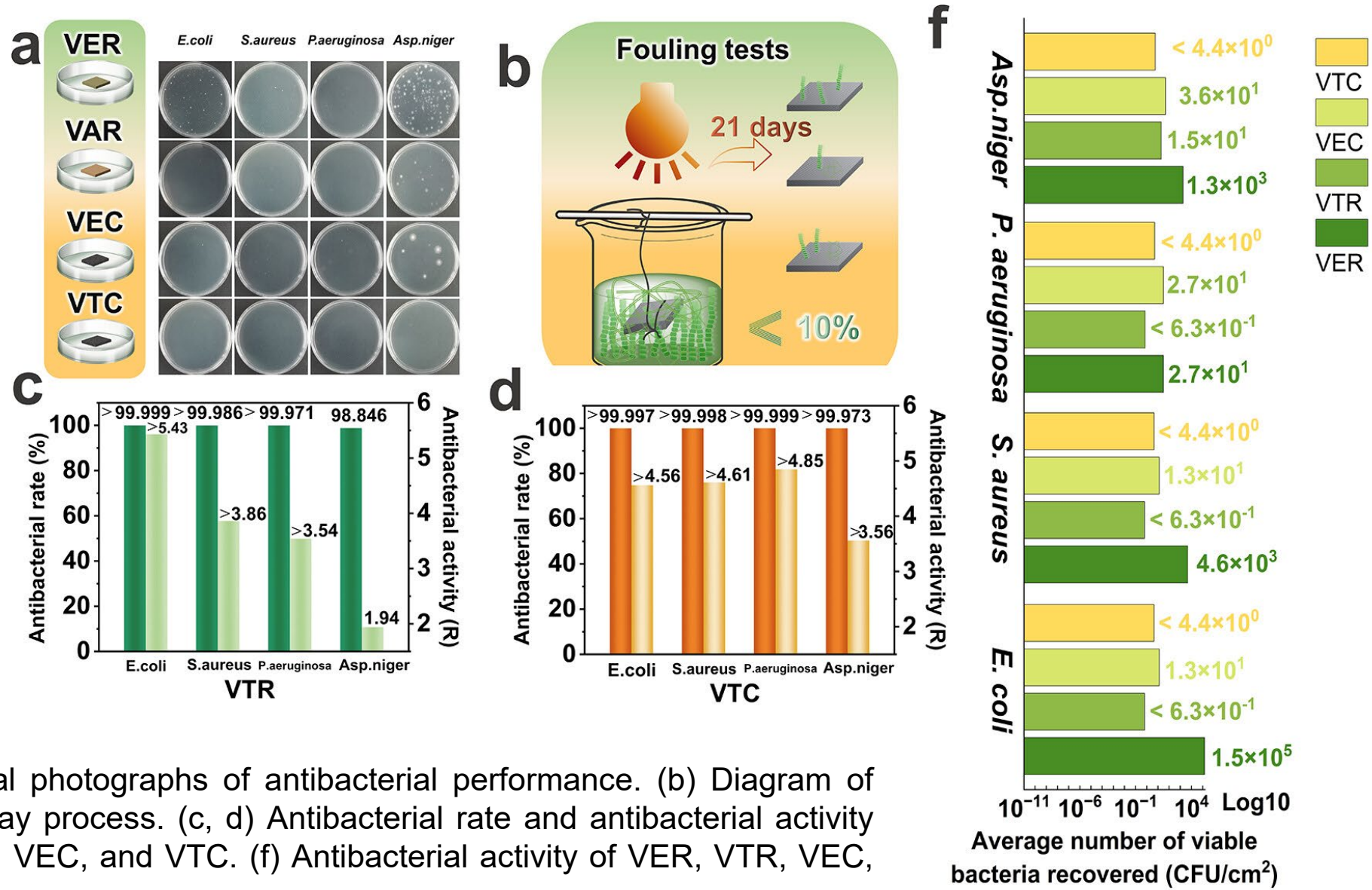

Fig: (a) Digital photographs of antibacterial performance. (b) Diagram of antialgae assay process. (c, d) Antibacterial rate and antibacterial activity of VER, VTR, VEC, and VTC. (f) Antibacterial activity of VER, VTR, VEC, and VTC.

Experimental data

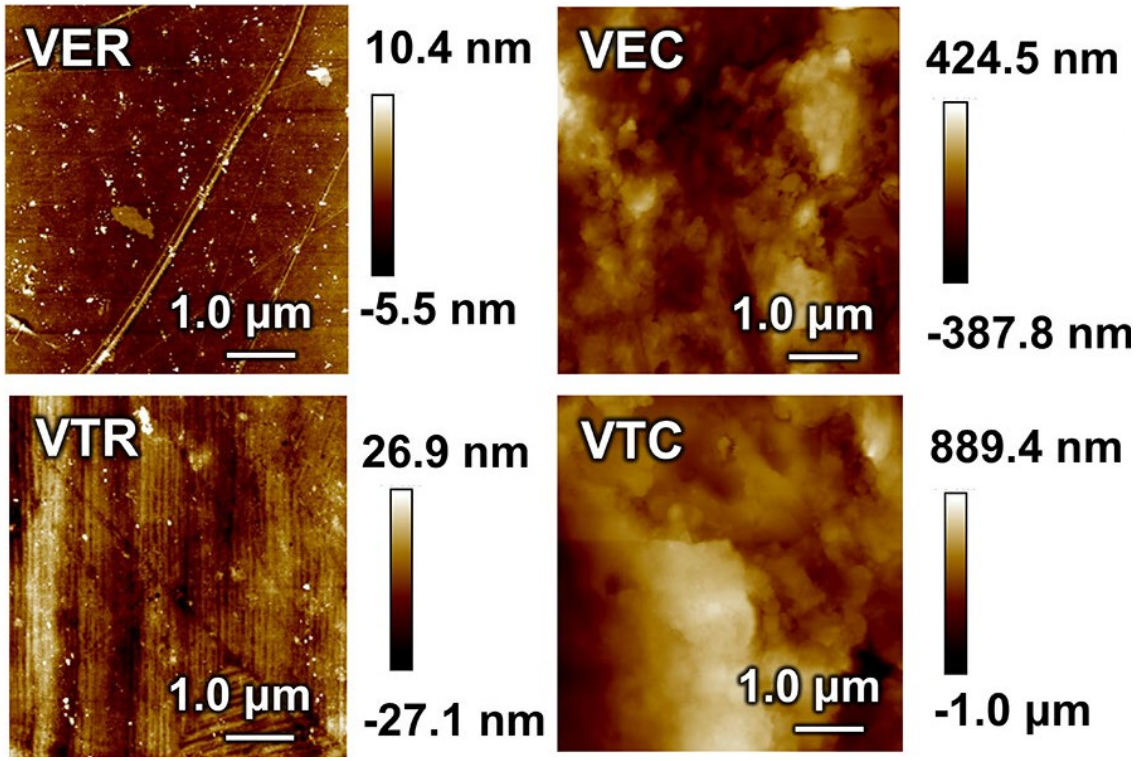

Fig: AFM height images of VER, VTR, VEC, and VTC surfaces.

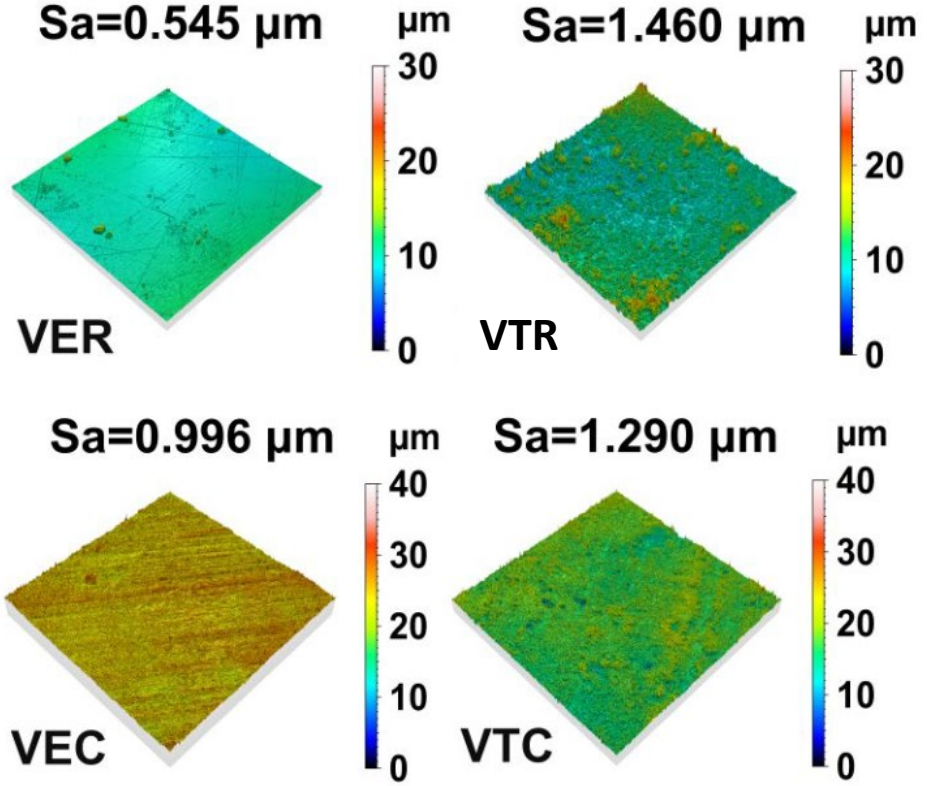

Fig: LSCM images of VER, VTR, VEC, and VTC surfaces.

Antimicrobial fouling mechanism

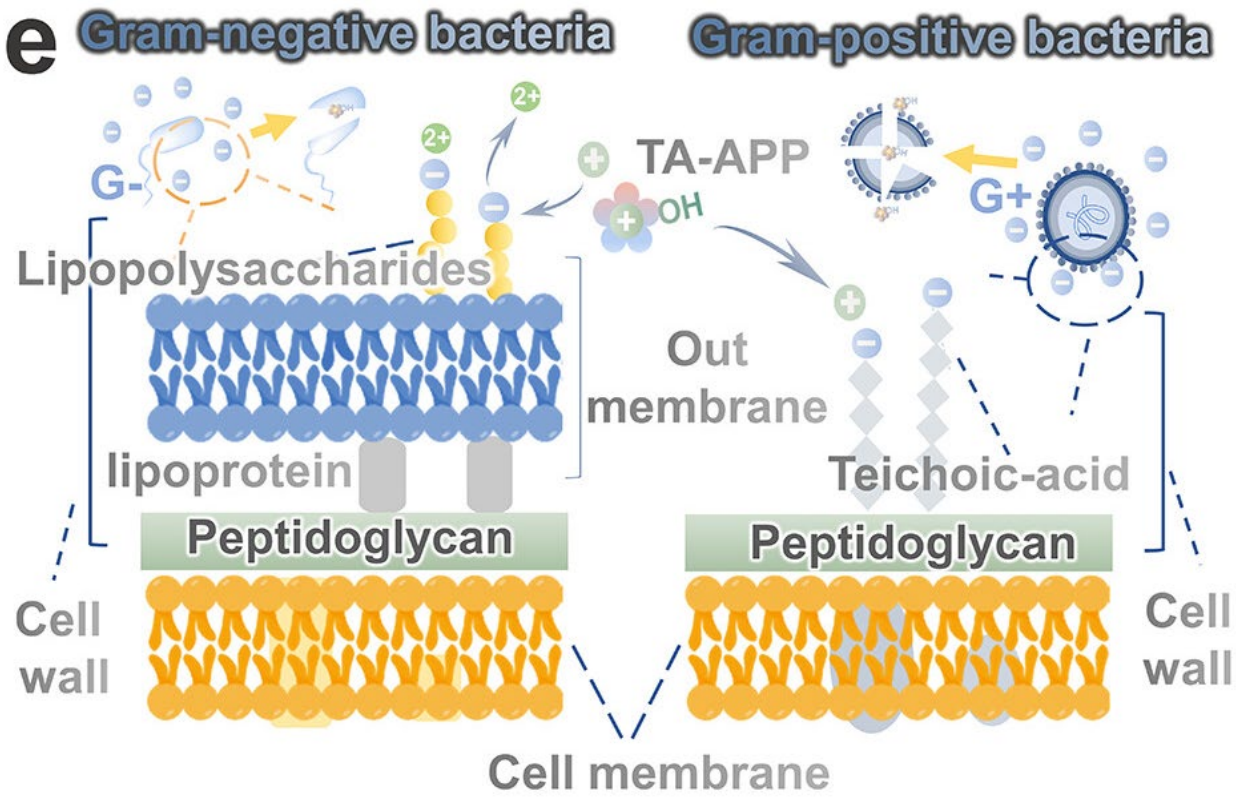

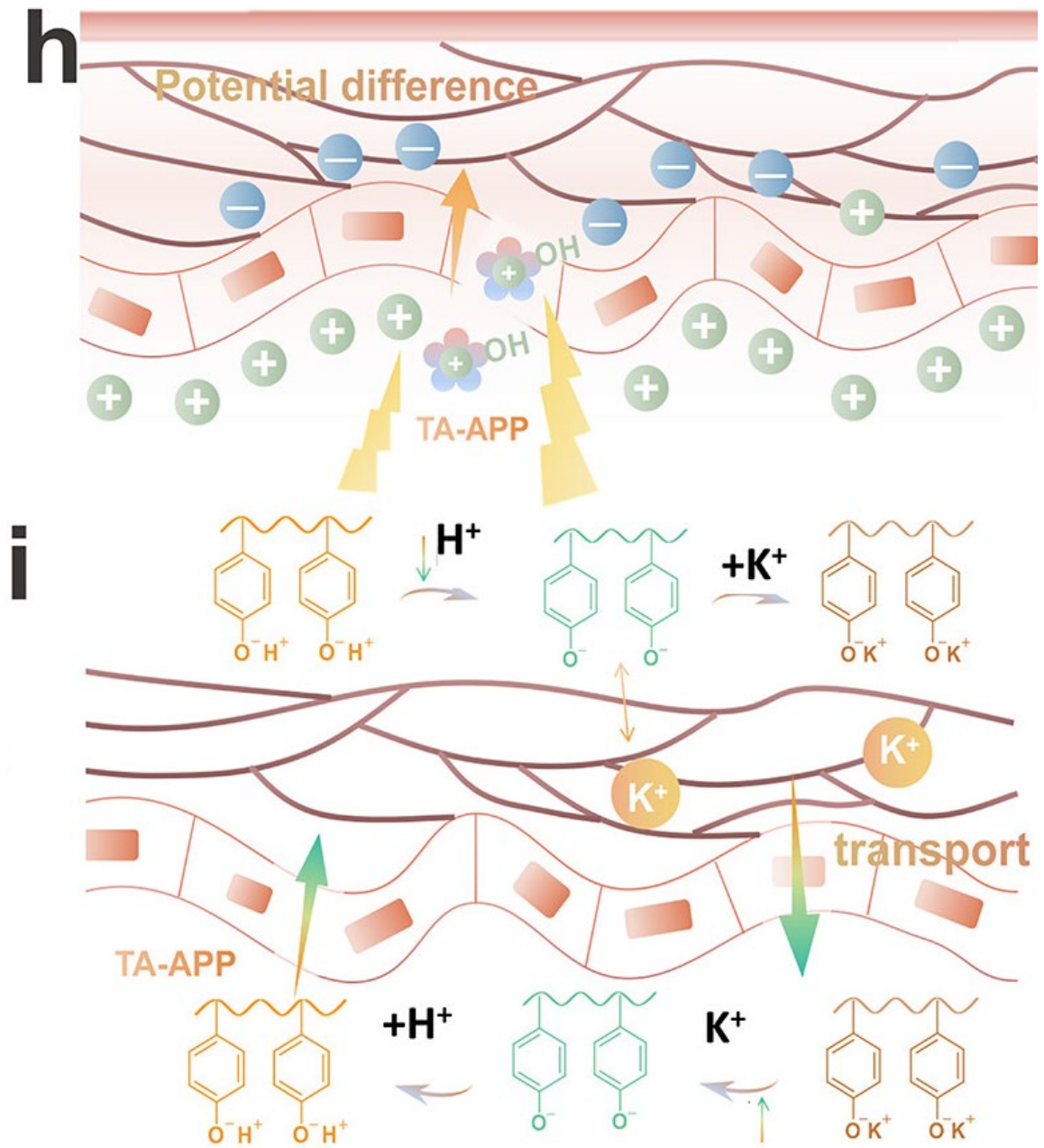

Fig: (e) Schematic diagram of the interaction of TA-APP with the cell wall and cell membrane of Gram-negative bacteria (G−) and Gram-positive bacteria (G+). (h) Bacterial cell destruction through electrical perforation caused by electrical potential difference. (i) Hydroxyl group accumulation causes damage to cytoplasmic membrane stability.

Experimental data

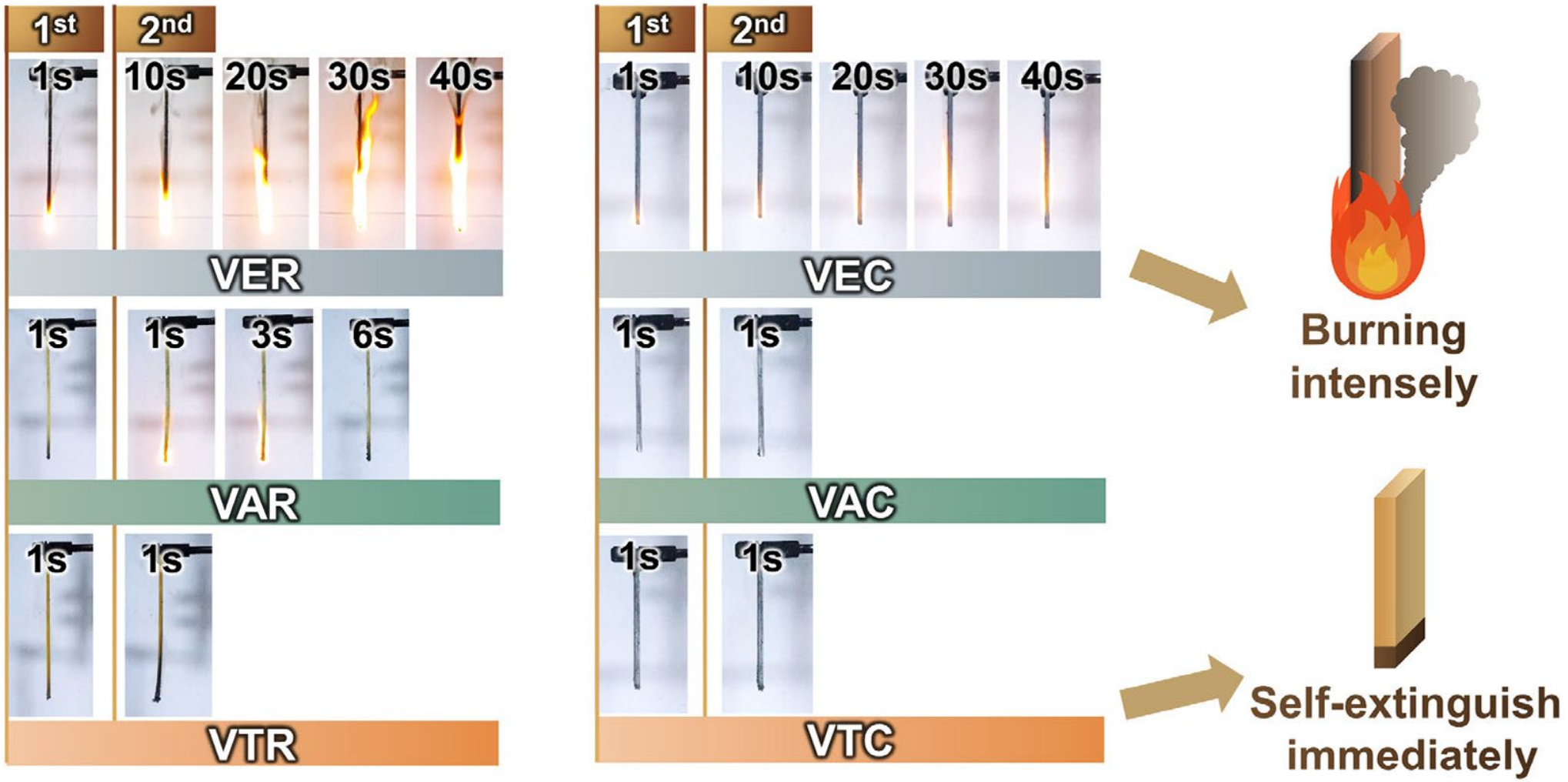

Fig: Vertical flame test (UL-94) digital photographs and burning performance illustrations.

Experimental data

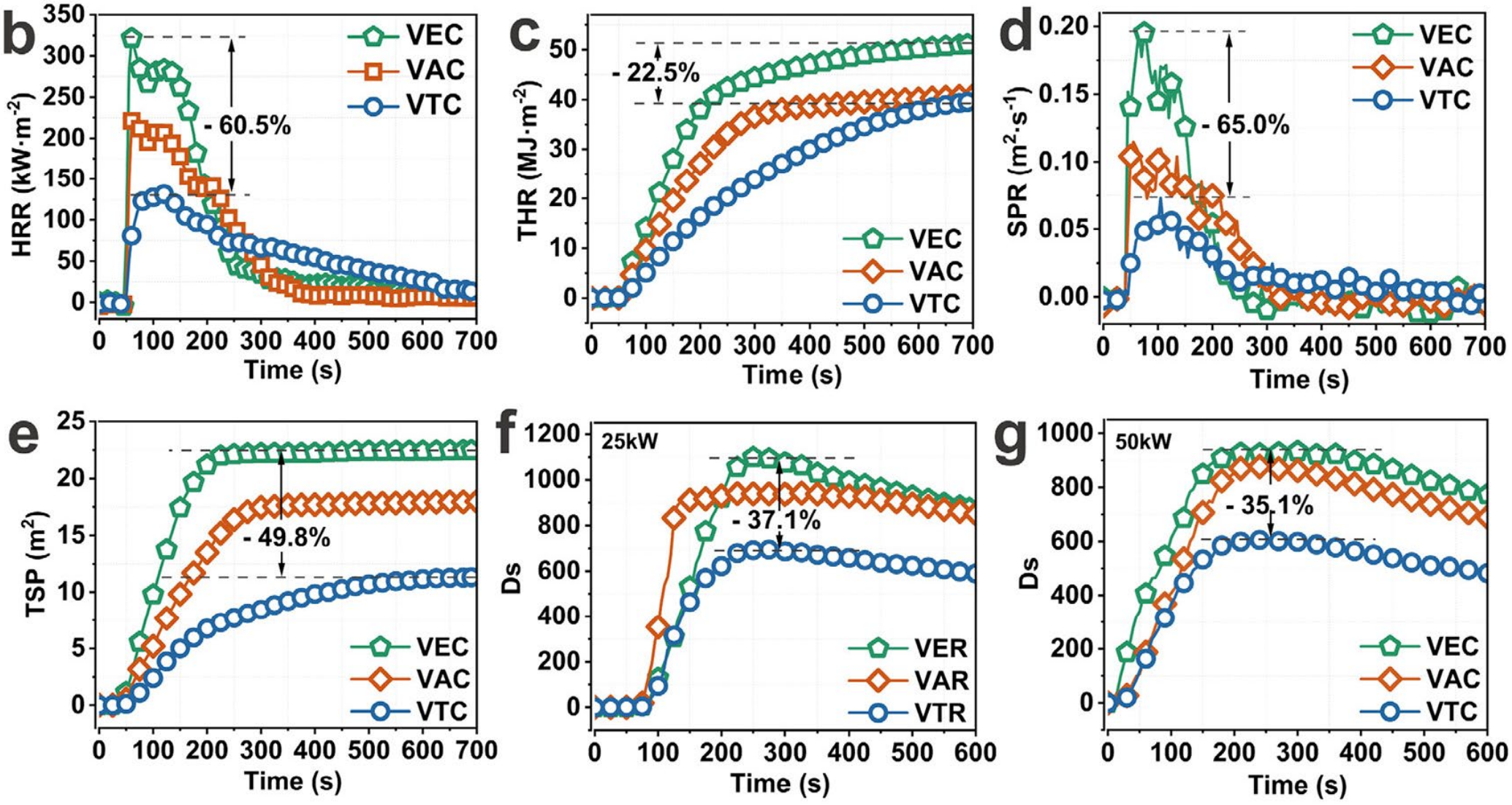

Fig: (b−e) HRR, THR, SPR, TSP curves in cone calorimetry test. (f, g) Smoke density curve.

Experimental data

Table S6. Data from cone calorimetry test of VER, VAR, VTR, VEC, VAC and VTC.

Samples	VER	VAR	VTR	VEC	VAC	VTC
TTI (s)	21	32	32	38	42	43
PHRR ($kW \cdot m^{-2}$)	859±5	532±5	296±9	333±9	236±10	131±6
Time to PHRR (s)	90	50	55	60	65	125
FIGRA($kW \cdot m^{-2}s^{-1}$)	9.5	10.6	5.4	5.6	3.6	1.1
THR ($MJ \cdot m^{-2}$)	88.2±0.6	57.1±0.6	59.2±0.1	51.0±8.1	40.9±5.0	39.5±8.1
Peak SPR ($m^2 \cdot s^{-1}$)	0.32±0.6	0.28±2.5	0.22±1.4	0.20±10.5	0.12±8.7	0.07±5.3
TSP (m^2)	36.3±7.4	29.0±3.5	30.1±4.2	22.5±3.2	18.0±2.0	11.3±4.8
Char mass (wt%)	0.1±2.0	34.3±2.3	32.0±0.6	51.4±5.8	64.3±4.7	64.4±4.4

Experimental data of the char

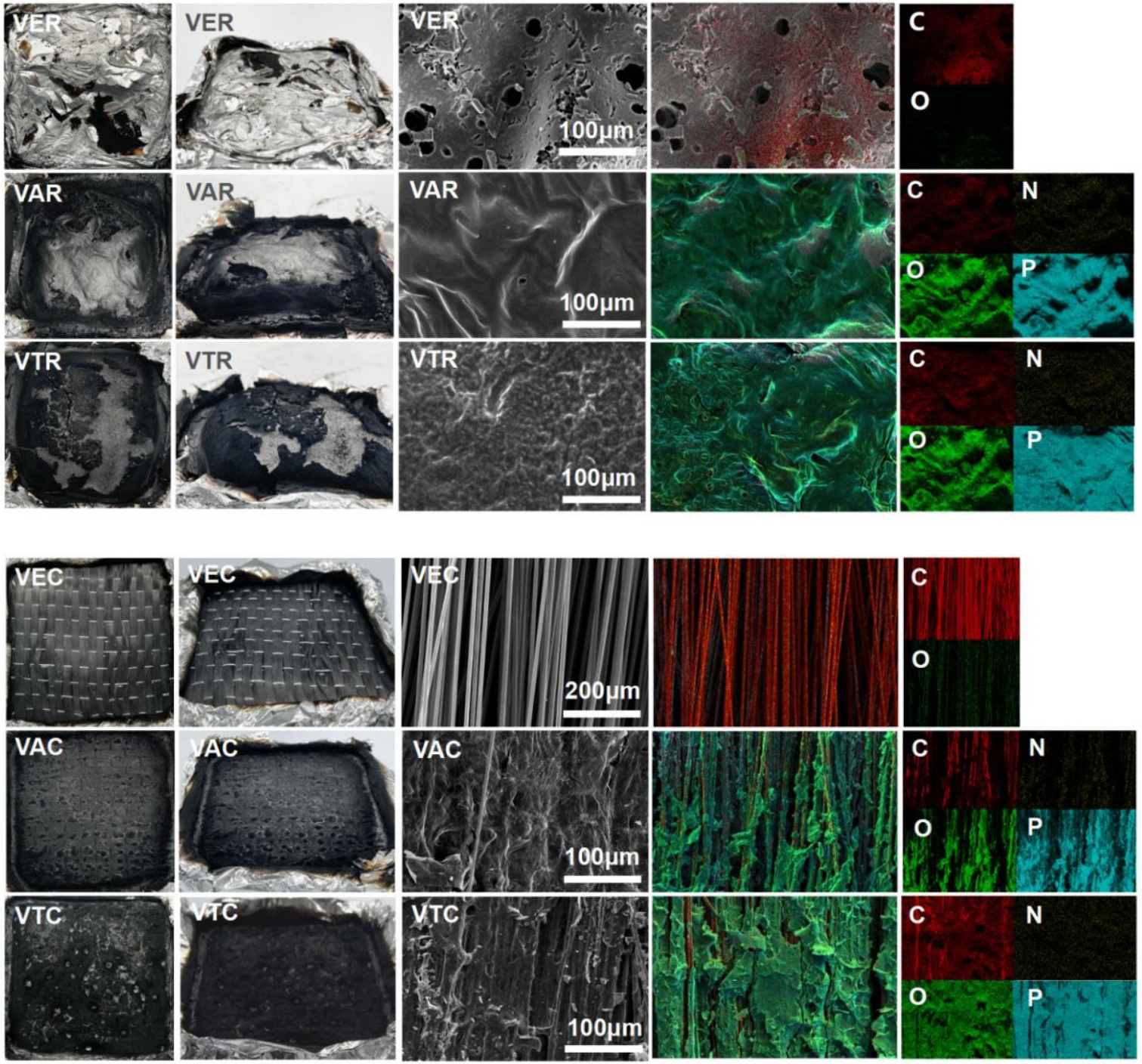

Fig: Digital photographs, SEM morphology micrographs and EDX elemental distribution mapping images

Experimental data of the char

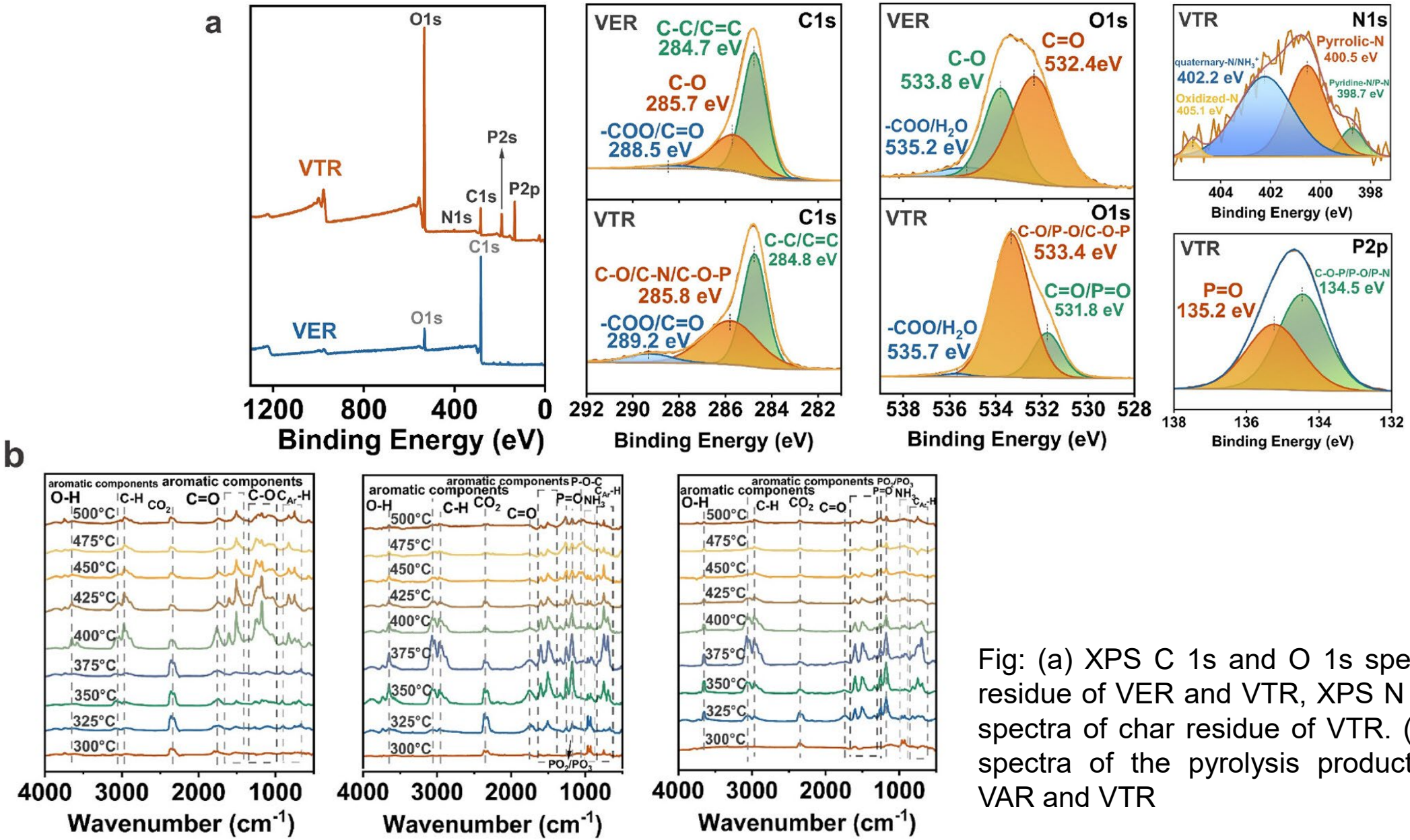

Fig: (a) XPS C 1s and O 1s spectra of char residue of VER and VTR, XPS N 1s and P2p spectra of char residue of VTR. (b) TG-FTIR spectra of the pyrolysis products for VER, VAR and VTR

Flame retardant mechanism

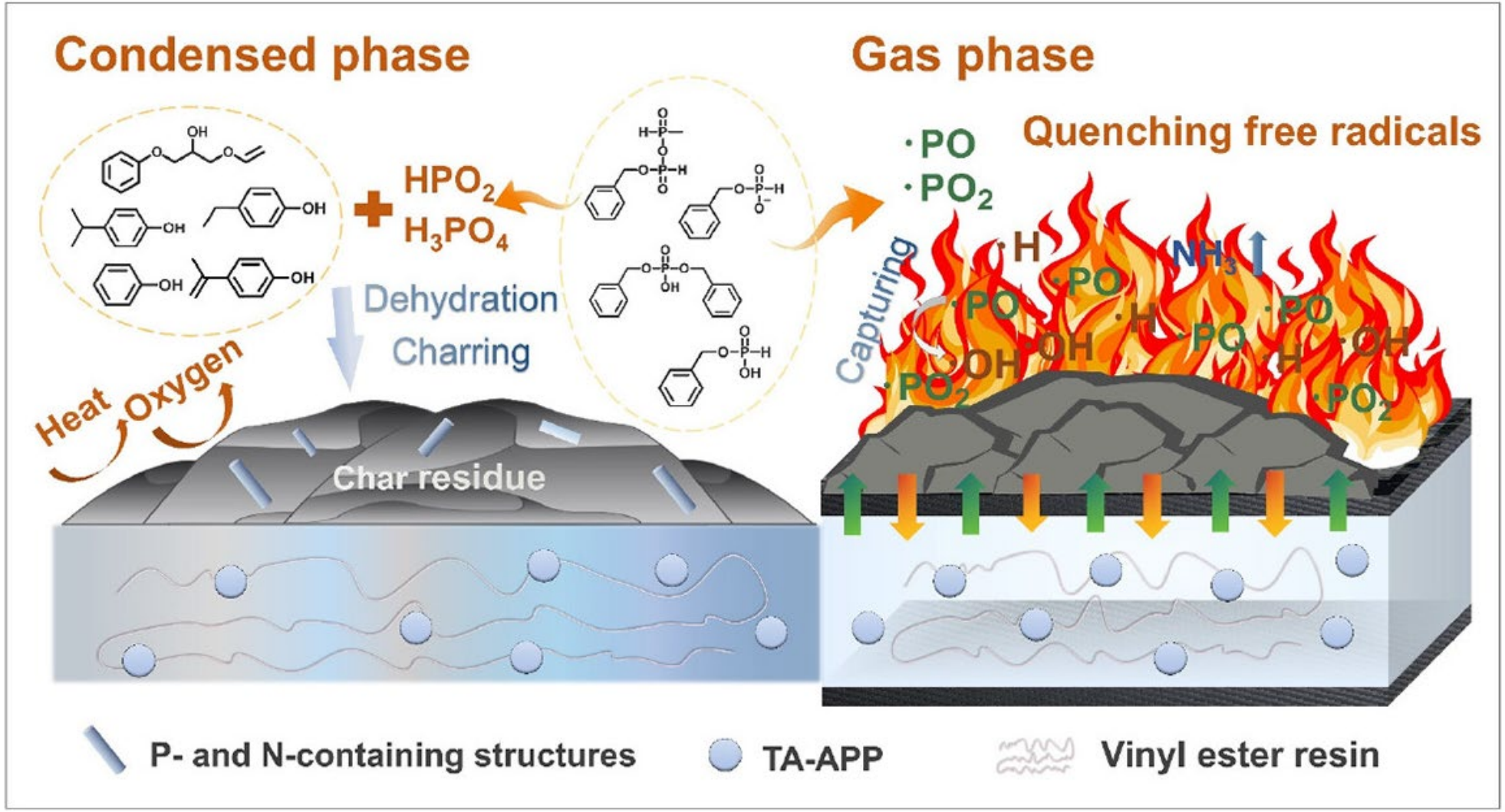

Conclusion

1. This work has developed a multifunctional substance, rich in ammonium phosphate and phenolic hydroxyl groups, providing flame-retardant, antibacterial, mold-proof, antialgal, and adhesive properties.
2. Combined with vinyl ester resin and carbon fibres to create a marine composite, mimicking sandcastle worms
3. Uses phenolic hydroxyl groups from tyramine to:
   - ✓ Enhance interfacial bonding force
   - ✓ Provide excellent antimicrobial fouling properties
4. Achieves high flame retardance through tyramine and ammonium phosphate synergy.
5. This work has developed a candidate for antimicrobial and fireproof protection in extreme ocean environments.